



Article

Low-Dose Ionizing Radiation Modulates Microglia Phenotypes in the Models of Alzheimer's Disease

Sujin Kim ^{1,†}, Hyunju Chung ^{2,†} , Han Ngoc Mai ³, Yunkwon Nam ¹, Soo Jung Shin ¹, Yong Ho Park ¹, Mi Joo Chung ³, Jong Kil Lee ⁴, Hak Young Rhee ⁵, Geon-Ho Jahng ⁶, Youngkyong Kim ⁷, Yu Jin Lim ⁷, Moonkyoo Kong ⁷ , Minhoo Moon ^{1,*} and Weon Kuu Chung ^{3,*}

¹ Department of Biochemistry, College of Medicine, Konyang University, 158, Gwanjeodong-ro, Seo-gu, Daejeon 35365, Korea; aktnfl3371@naver.com (S.K.); yunkwonnam@gmail.com (Y.N.); tlstnzz83@gmail.com (S.J.S.); znf900809@naver.com (Y.H.P.)

² Department of Core Research Laboratory, Medical Science Research Institute, Kyung Hee University Hospital at Gangdong, Seoul 05278, Korea; hjchung@khu.ac.kr

³ Department of Radiation Oncology, Kyung Hee University Hospital at Gangdong, Seoul 05278, Korea; maingochan244@gmail.com (H.N.M.); mjwithu@khnmc.or.kr (M.J.C)

⁴ Department of Pharmacy, College of Pharmacy, Kyung Hee University, Seoul 02447, Korea; jklee3984@gmail.com

⁵ Department of Neurology, Kyung Hee University Hospital at Gangdong, Seoul 05278, Korea; azzo73@gmail.com

⁶ Department of Radiology, Kyung Hee University Hospital at Gangdong, Seoul 05278, Korea; ghjahng@gmail.com

⁷ Department of Radiation Oncology, Kyung Hee University Medical Center, Kyung Hee University School of Medicine, Seoul 02447, Korea; icarus070@hanmail.net (Y.K.); yujindw@naver.com (Y.J.L.); kongmoonkyoo@khu.ac.kr (M.K.)

* Correspondence: hominmoon@konyang.ac.kr (M.M.); wkchung@khnmc.or.kr (W.K.C.); Tel.: +82-42-600-8691 (M.M.); +82-2-440-6071 (W.K.C.)

† These authors contributed equally to this work.

Received: 30 March 2020; Accepted: 24 June 2020; Published: 25 June 2020



Abstract: Alzheimer's disease (AD) is the most common type of dementia. AD involves major pathologies such as amyloid- β ($A\beta$) plaques and neurofibrillary tangles in the brain. During the progression of AD, microglia can be polarized from anti-inflammatory M2 to pro-inflammatory M1 phenotype. The activation of triggering receptor expressed on myeloid cells 2 (TREM2) may result in microglia phenotype switching from M1 to M2, which finally attenuated $A\beta$ deposition and memory loss in AD. Low-dose ionizing radiation (LDIR) is known to ameliorate $A\beta$ pathology and cognitive deficits in AD; however, the therapeutic mechanisms of LDIR against AD-related pathology have been little studied. First, we reconfirm that LDIR (two Gy per fraction for five times)-treated six-month 5XFAD mice exhibited (1) the reduction of $A\beta$ deposition, as reflected by thioflavins S staining, and (2) the improvement of cognitive deficits, as revealed by Morris water maze test, compared to sham-exposed 5XFAD mice. To elucidate the mechanisms of LDIR-induced inhibition of $A\beta$ accumulation and memory loss in AD, we examined whether LDIR regulates the microglial phenotype through the examination of levels of M1 and M2 cytokines in 5XFAD mice. In addition, we investigated the direct effects of LDIR on lipopolysaccharide (LPS)-induced production and secretion of M1/M2 cytokines in the BV-2 microglial cells. In the LPS- and LDIR-treated BV-2 cells, the M2 phenotypic marker CD206 was significantly increased, compared with LPS- and sham-treated BV-2 cells. Finally, the effect of LDIR on M2 polarization was confirmed by detection of increased expression of TREM2 in LPS-induced BV2 cells. These results suggest that LDIR directly induced phenotype switching from M1 to M2 in the brain with AD. Taken together, our results indicated that LDIR modulates LPS- and $A\beta$ -induced neuroinflammation by promoting M2 polarization via TREM2 expression, and has beneficial effects in the AD-related pathology such as $A\beta$ deposition and memory loss.

Keywords: low-dose ionizing radiation; microglia; amyloid-beta; Alzheimer's disease; TREM2, M1/M2

1. Introduction

Alzheimer's disease (AD) is the most common cause of dementia and characterized the accumulation of extracellular amyloid- β ($A\beta$) plaques and insoluble intracellular neurofibrillary tangles in the brain [1]. $A\beta$ is the most important pathogenic factor for the development of AD, and causes several pathological changes, including memory loss, neuroinflammation, synaptic loss, and neuronal cell death [2]. In particular, $A\beta$ -induced neuroinflammation is known to accelerate AD progression through neuronal damage induced by expression of inflammatory mediators [3,4]. Similarly, it has been known that lipopolysaccharides (LPS)-provoked neuroinflammation can also cause synaptic loss and induce cognitive impairment in AD [5,6]. In addition, LPS-mediated inflammation might be associated with enhancement of $A\beta$ production [5,7,8]. Thus, both $A\beta$ and LPS are one of the cause factors for the pathogenesis of AD by inducing neuroinflammation [5,9,10].

The microglia, which are the innate immune effector cells in central nervous system, have dual conflicting roles, such as neurotoxic and neuroprotective action, in the pathogenesis of neurodegenerative diseases, and these roles are associated with different functional phenotypes of microglia: M1 and M2 [11–13]. Switching of the microglial phenotype to M1 or M2 is regulated by pathological conditions. Toxins bind to the microglia cell surface and activate the M1 phenotype, which then produces neurotoxic cytokines [14,15]. Thus, persistent or unregulated neuroinflammation can cause tissue damage and secondary injury [16,17]. Conversely, M2 anti-inflammatory microglia promote tissue remodeling and repair by releasing anti-inflammatory cytokines [15,18]. Therefore, suppressing M1 microglial polarization which is subsequent release of pro-inflammatory molecules and/or enhancing the secretion of beneficial anti-inflammatory molecules from M2-polarized microglial cells could be a potential therapeutic approach for the treatment of AD [19,20].

Triggering receptor expressed on myeloid cells 2 (TREM2) is a type of membrane protein present on the surface of microglia and plays key roles in proliferation and survival of microglia, and secretion of inflammatory cytokines from microglia [21]. In the BV-2 microglial cell, knockdown of TREM2 induces the polarization to M1 phenotype, and overexpression of TREM2 promotes shifting to M2 phenotype of microglia [22]. Interestingly, TREM2 is known to be essential for microglia to recognize and phagocytose the $A\beta$ in the brain with AD [23]. In addition, it has been known that TREM2 may be activated by various ligands, such as $A\beta$, LPS, apolipoproteins, and lipoproteins [24,25]. Moreover, TREM2 expression is decreased by pro-inflammatory stimuli, such as tumor necrosis factor alpha (TNF- α), interleukin-1 beta (IL-1 β), or LPS [26–28]. Furthermore, knockdown of TREM2 in microglia suppresses phagocytic activity and activates gene transcription of TNF- α , whereas overexpression of TREM2 in microglia not only promotes phagocytosis but also diminishes pro-inflammatory responses [29]. Particularly, it was shown that up-regulated TREM2 expression in the 5XFAD mice reduced $A\beta$ plaque and neurite dystrophy, and improved cognitive function and promoted microglial phagocytosis [30]. Furthermore, a number of studies have shown that TREM2 is related with microglial phenotype switching in neurological disorders, including AD [22,31–34]. Taken together, it can be suggested that microglia polarization might be associated with the TREM2 in the microglia within AD brain.

Although some of studies demonstrated that the low-dose ionizing radiation (LDIR) shows negative impacts on neurogenic precursor populations, dendritic spine density and cognitive dysfunction [35–37], several studies demonstrated that LDIR could be an effective intervention for the treatment of AD [38–41]. A number of reports have shown that LDIR significantly influences cognitive improvement and memory loss in AD [42–45]. In addition, it has been reported that ionizing radiation to the brain reduces deposition of $A\beta$ plaque in $A\beta$ -overexpressing transgenic models of AD [45]. Furthermore, LDIR decreases pro-inflammatory cytokines, such as interferon-gamma

(INF- γ) and TNF- α , in animal models of AD [45,46]. However, there has been no studies about (1) the mechanisms how the radiation therapy reduces the A β accumulation and cognitive deficit in AD, and (2) the effect of LDIR therapy on M1/M2 polarization of microglia.

In this perspective, we hypothesized that LDIR-exposure would modulate the polarization of microglia phenotype and the expression of TREM2, resulting in amelioration of A β deposition and cognitive decline in AD. We found that LDIR affects microglial phenotype changes and the up-regulation of TREM2 in the LPS-treated microglia cell and A β -overexpressing mice. In this study, we demonstrated that LDIR causes the phenotype switching, which finally attenuated A β deposition and cognitive decline in AD.

2. Results

2.1. LDIR Inhibits A β Deposition and Improved Cognitive Deficits in 5XFAD Mice

It has been known that LDIR reduces the number of amyloid plaques and plaques size [43,45], and improves cognitive decline in the animal models of AD [44,45,47]. We reaffirmed the effect of the LDIR on A β deposition and cognitive function in the 5XFAD mice after exposure to 10 Gy radiation over 5 days (Figure 1A). We performed Morris water maze used in the previous studies, which demonstrated the alleviatory effect of LDIR on cognitive decline at 8 weeks after radiation therapy [44,45]. To confirm whether the LDIR inhibits A β aggregation in the cerebral cortex and hippocampus, brain sections were labeled by thioflavin S staining (Figure 1B). In comparison to sham-treated 5XFAD mice, LDIR-treated 5XFAD mice exhibited significant decrease in A β -positive area in both cerebral cortex and hippocampus (Figure 1C). To further reconfirm whether LDIR effectively rescues cognitive dysfunction in AD, Morris water maze test was performed with 5XFAD mice. The representative swimming paths of mice in each group indicated that the sham-treated AD transgenic model mice performed more unnecessary swimming (Figure 1D). The LDIR-treated 5XFAD mice showed increase in the quadrant time compared to sham-treated 5XFAD mice (Figure 1F). Particularly, two-way ANOVA repeated measures with multiple comparisons revealed a significant decrease in the escape latency on day 7 and 8 of trials in the LDIR-treated 5XFAD group compared with sham-treated 5XFAD group (Figure 1E). Consistent with previous reports, our results indicated that LDIR treatment ameliorates the A β accumulation and cognitive impairment in the A β -overexpressing transgenic mice.

2.2. LDIR Regulates A β -Induced Production of Inflammatory Cytokines in the 5XFAD Mice

It has been shown that LDIR exposure reduces the neuroinflammation in animal models of AD [41,45,46]. Inhibition of the M1 pro-inflammatory cytokines secreted from glial cells has been shown to attenuate synaptic dysfunction and enhance cognitive function in the AD [48]. In addition, activation of the M2 phenotype and inhibition of the M1 phenotype increased A β phagocytosis and clearance of amyloid plaques [49]. Therefore, we examined whether LDIR-induced improvement of cognitive function and reduction of A β deposition might be mediated by switching phenotype of microglial cells. To elucidate whether the LDIR may regulate microglial cytokine productions, representative cytokines of M1 and M2 microglia were examined in 5XFAD brain samples using qRT-PCR. We quantified mRNA levels of M1 pro-inflammatory marker TNF- α and M2 anti-inflammatory marker TGF- β in the brains of sham- and LDIR-treated 5XFAD mice. The levels of TNF- α mRNA were reduced in LDIR-treated 5XFAD compared to sham-treated 5XFAD mice (Figure 2A). In contrast, the levels of TGF- β mRNA were significantly increased in LDIR-treated 5XFAD compared to sham-treated 5XFAD mice (Figure 2B). Our results suggest that the M2 cytokine was up-regulated, and the M1 cytokine was suppressed after LDIR therapy in the brain of 5XFAD mice.

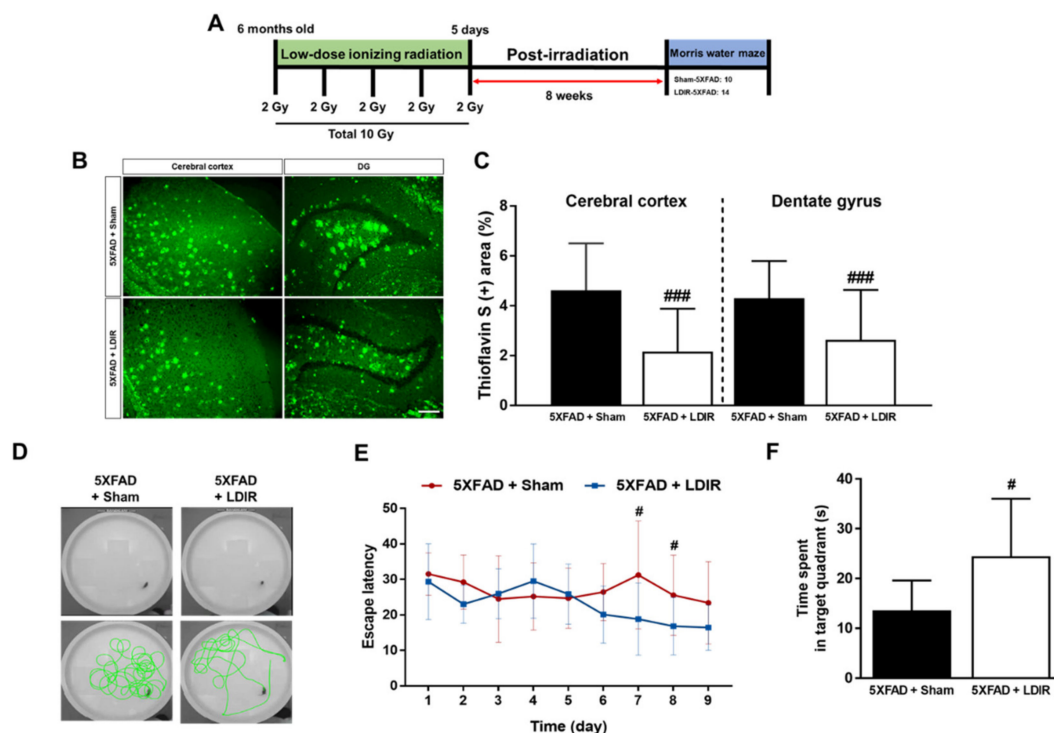


Figure 1. The inhibitory effects of low-dose ionizing radiation (LDIR) therapy on amyloid- β ($A\beta$) accumulation and cognitive dysfunction in 5XFAD mice. (A) Schematic diagram of the experimental procedure. (B) Histochemical staining for thioflavin S was performed to identify amyloid plaques in the cerebral cortex and hippocampal dentate gyrus (DG) of the sham- and LDIR-treated 5XFAD mice (scale bar = 250 μ m). (C) $A\beta$ -positive areas in the cerebral cortex and dentate gyrus of the sham- and LDIR-treated 5XFAD mice were quantified and plotted as a percentage. (D) Representative of swimming paths was recorded on videotape during the test session of the Morris water maze. (E) Latency to escape time of the mice was measured. Repeated-measures two-way ANOVA with Fisher’s post hoc test compared to 5XFAD+Sham mice. (F) Measurement of quadrant time to spend in the hidden platform. Data are presented as mean \pm SD (n = 10 mice in sham-treated 5XFAD mice and n = 14 mice in LDIR-treated 5XFAD mice). # p < 0.05 and ### p < 0.001 indicate significant differences between the sham- and LDIR-exposed 5XFAD mice.

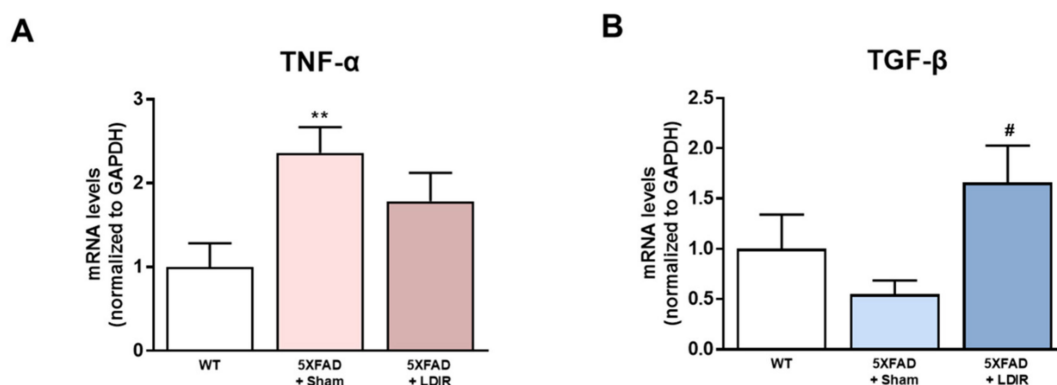


Figure 2. The modulatory effects of LDIR on production of M1/M2 cytokines in the brain of 5XFAD mice. (A) Level of TNF- α mRNA was checked by qRT-PCR. (B) Level of TGF- β mRNA was measured by qRT-PCR. ** p < 0.01 indicate significant differences between the wild-type (WT) and sham-treated 5XFAD mice. # p < 0.05 indicate significant differences between the sham- and LDIR-treated 5XFAD mice. Data are presented as mean \pm SD (n = 3 mice each group).

2.3. LDIR Modulates the Levels of M1/M2 Cytokines in LPS-Treated BV-2 Cells

To confirm the direct effect of the LDIR on microglia polarization with M1/M2 phenotype in the AD brain, we selected the BV-2 cell, which is an immortalized neonatal mouse microglial cell line. First, to identify the cytotoxicity of LPS, the BV-2 cells were incubated with LPS at concentrations of 1, 10, 20, 100, 1000, and 2000 ng/mL for 24 h (Figure 3B). The concentrations of LPS and culture conditions tested were based on previous studies [50–52]. We aimed to determine the optimal concentration of LPS, which changed the mRNA levels of M1 and M2 cytokines in microglia but was the least toxic to these cells (Figure 3B–D). As depicted in Figure 3B, treatment with LPS for 24 h was not toxic to the cells. In addition, we also observed that various doses of LDIR exposure did not cause the toxicity of BV-2 cells (Figure S1). As shown in Figures 3C and 3D, there was a significant change in the mRNA levels of M1 and M2 cytokines after LPS treatment. An amount of 20 ng/mL was chosen as a standard concentration for further experiments. The BV-2 cells were treated with LPS at a dose of 20 ng/mL and exposed to 1 Gy radiation for 1 fraction (Figure 3A). Expression levels of M1 cytokines (TNF- α , IL-1 β and IL-6) and M2 cytokines (TGF- α , TGF- β and IL-10) were measured by qRT-PCR to assess the phenotype switching in BV-2 cells. After 24 h of LPS treatment, mRNA levels of M1 cytokines were markedly elevated (Figure 3E), while mRNA levels for M2 cytokines were dramatically reduced when compared to the control group (Figure 3F). However, LDIR treatment significantly reduced mRNA levels of M1 cytokines (Figure 3E) and elevated the mRNA levels of M2 cytokines (Figure 3F), indicating that the LPS-treated BV-2 cells revealed phenotype switching from M1 to M2 following LDIR treatment. Subsequently, in addition to mRNA levels of M1/M2 cytokines, we also measured the released M1/M2 cytokines from LPS-treated BV-2 cells without or with LDIR using ELISA. Secretion of M1 pro-inflammatory cytokines, such as TNF- α , IL-1 β , and IL-6, into the culture medium of BV-2 cells dramatically increased in response to LPS stimulation (Figure 3G). However, after LDIR, the release of M1 cytokines was significantly inhibited in LPS-stimulated microglia (Figure 3G). In addition, the production of M2 cytokines, such as TGF- β and IL-10, from LPS-treated BV-2 cells were significantly induced 24 h after LDIR (Figure 3H). Taken together, these data suggested that LDIR could effectively shift the LPS-induced M1 phenotype to an M2 phenotype of microglial cells.

2.4. LDIR Affects Changes of M1/M2 Phenotypes of LPS-Treated BV-2 Cells

Using the markers for M1 and M2 microglial phenotype [53–55], we tried to clearly demonstrate that LDIR can change the polarization of M1/M2 activation of LPS-treated microglial cells. We examined the expression of BV-2 cell surface receptors: M1 phenotypic marker CD86 and M2 phenotypic marker CD206. At the mRNA levels, the LPS or LDIR alone did not induce the inflammatory response on BV-2 cells compared with control group. In addition, there were no changes of CD86 in the LPS-treated BV-2 cells 12 and 24 h after LDIR exposure (Figure 4A). On the other hand, there were significant up-regulation of CD206 in the LPS-stimulated BV-2 cells 12 and 24 h after LDIR exposure (Figure 4B). We demonstrated that M2 polarization of microglia can be induced by LPS+LDIR treatment.

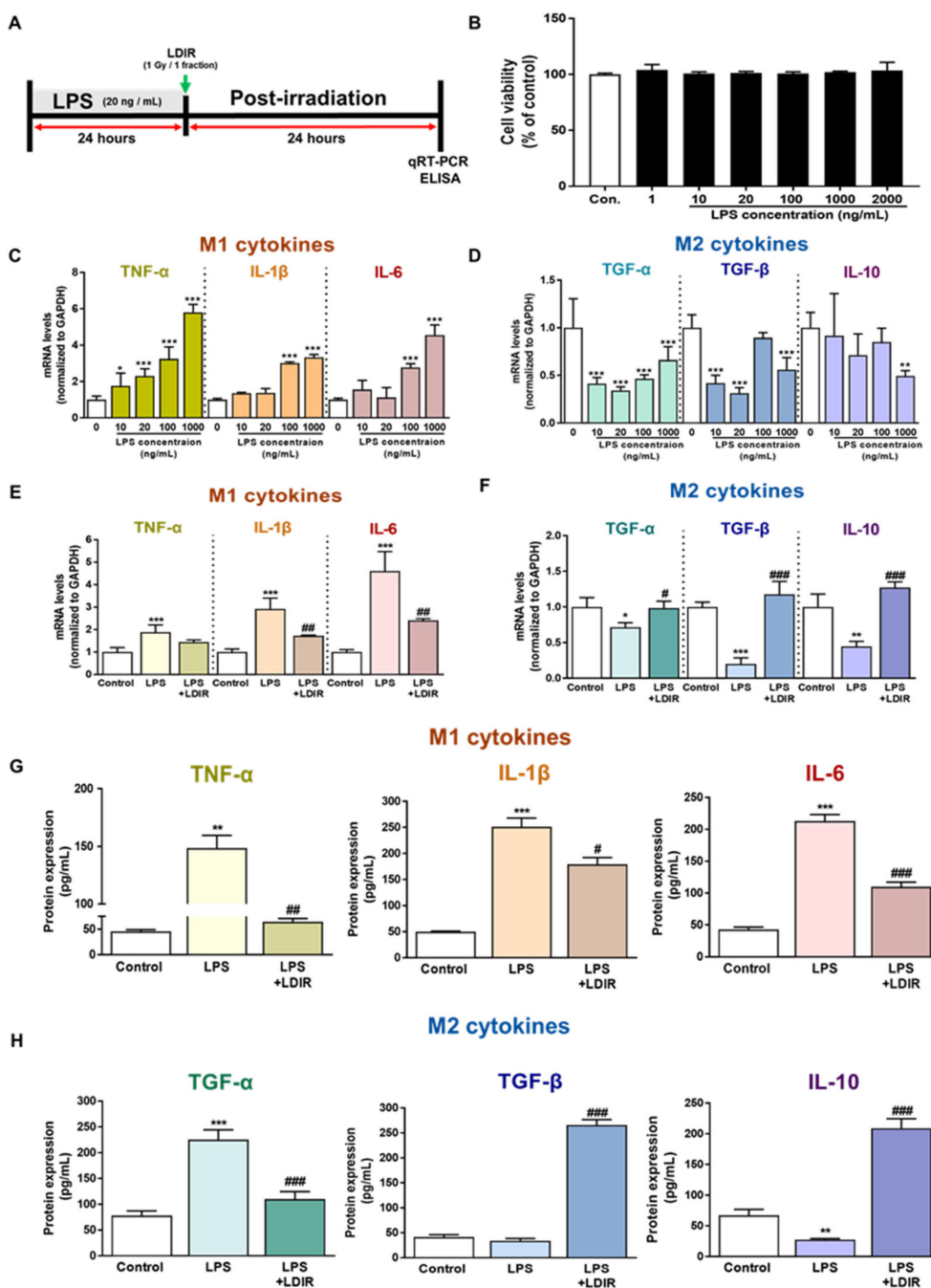


Figure 3. The modulatory effects of LDIR on production and secretion of M1 cytokines (TNF- α , IL-1 β and IL-6) and M2 cytokines (TGF- α , TGF- β and IL-10) in lipopolysaccharide (LPS)-treated BV-2 cells. (A) Outline of the experimental design for in vitro assessment. (B) BV-2 cells were treated with LPS at doses of 1, 10, 20, 100, 1000 and 2000 ng/mL for 24 h. Cell viability was determined by the cell counting Kit-8 assay. (C,D) After BV-2 cells were treated with LPS (10, 20, 100, and 1000 ng/mL) for 24 h, the mRNA expression levels of M1 cytokines and M2 cytokines were measured by qRT-PCR. (E–H) BV-2 cells were treated with LPS (20 ng/mL) for 24 h, then exposed to LDIR (1 Gy/1 fraction). The mRNA expression levels of (E) M1 cytokines and (F) M2 cytokines were measured by qRT-PCR. The protein levels of (G) M1 cytokines and (H) M2 cytokines in cultured media were measured by ELISA. * $p < 0.05$, ** $p < 0.01$, and *** $p < 0.001$ indicate significant differences between the control and LPS-treated group. # $p < 0.05$, ## $p < 0.01$, and ### $p < 0.001$ indicate significant differences between the LPS- and LPS + LDIR- treated group. Data are presented as mean \pm SD from triplicate experiments.

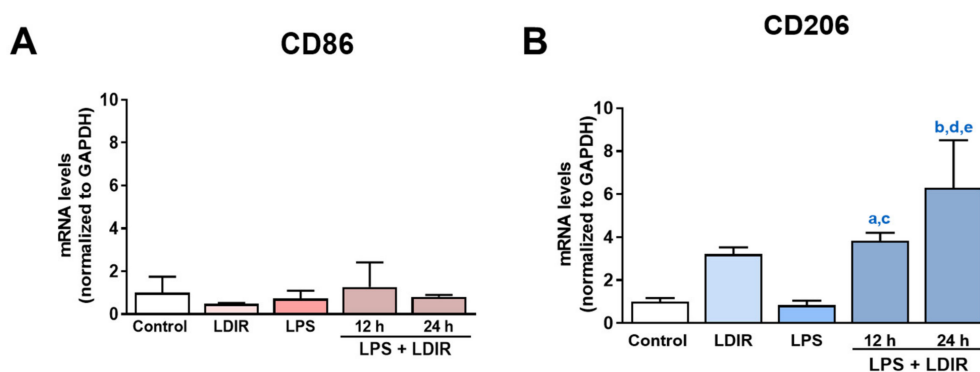


Figure 4. The effects of LDIR exposure on the expressions of M1/M2 markers in BV-2-stimulated cells. BV-2 cells were treated with LPS at a dose of 20 ng/mL for 24 h then exposed to LDIR (1 Gy/ 1 fraction). Cells were harvested at 12 and 24 h after irradiation. (A,B) The mRNA levels of M1 microglial marker CD86 and M2 microglial marker CD206 were measured by qRT-PCR. a indicated that comparison of control and LPS+LDIR 12 h ($p < 0.05$), b indicated that comparison of control and LPS+LDIR 24 h ($p < 0.001$), c indicated that comparison of LPS and LPS+LDIR 12 h ($p < 0.05$), d indicated that comparison of LPS and LPS+LDIR 24 h ($p < 0.001$), and e indicated that comparison of LDIR and LPS+LDIR 24 h ($p < 0.05$). Data are presented as mean \pm SD from triplicate experiments.

2.5. LDIR Induces the Up-Regulation of TREM2 in LPS-Treated BV-2 Cells

TREM2, one of microglial transmembrane receptors, is known as a regulator of the microglial M1/M2 polarization and microglial responsivity in AD [22,30]. We examined whether the LDIR may affect the expression of TREM2 in microglia showing polarization to M2 phenotype. We found the LDIR-mediated up-regulation of TREM2 mRNA level in BV-2 cells, compared with control groups. Furthermore, LPS-treated BV-2 cells exposed to LDIR showed significant up-regulation of TREM2 mRNA in BV-2 cells, compared with LPS-treated groups (Figure 5). Taken together, our data suggest that LDIR treatment could simultaneously induce M2 polarization of microglia and the upregulation of TREM2 in activated microglia.

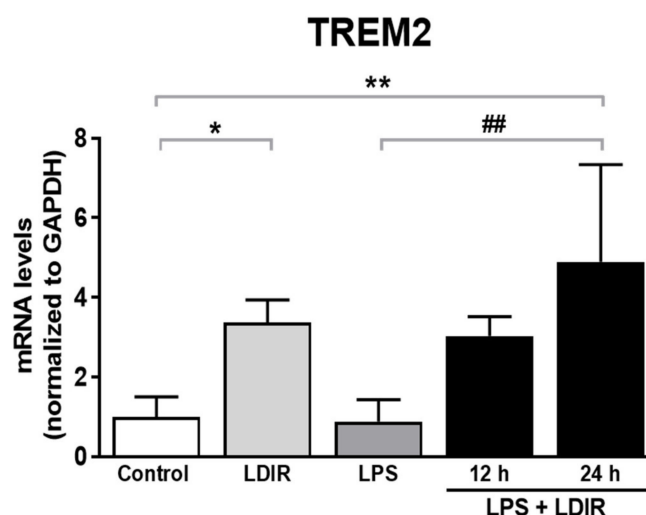


Figure 5. The enhancing effects of LDIR exposure on expression of TREM2 in LPS-stimulated BV-2 cells. BV-2 cells were treated with LPS at a dose of 20 ng/mL for 24 h, and then were exposed to LDIR (1 Gy/ 1 fraction). Cells were harvested at 12 and 24 h after irradiation. After irradiation and/or LPS treatment, levels of TREM2 mRNA were detected by qRT-PCR in BV-2 cells. * $p < 0.05$, ** $p < 0.01$ indicate significant differences to control group. ## $p < 0.01$ indicate significant differences to LPS group. Data are presented as mean \pm SD from triplicate experiments.

3. Discussion

Recently, studies about LDIR exposure for the treatment of AD have been increasing [38,39]. Although previous studies have reported the beneficial effect of the LDIR therapy on the A β pathology and cognitive decline in AD [43,45], there has been few studies about the mechanism of the LDIR therapy for the treatment of AD. Therefore, we examined the effects of the LDIR on microglial phenotypes and expression of TREM2 in AD models. Consistent with previous reports, our results also revealed that LDIR inhibits A β deposition and cognitive dysfunction in 5XFAD mice (Figure 1). Intriguingly, exposure to LDIR regulated the expression of pro-inflammatory and anti-inflammatory cytokines in the brain of A β -overexpressing transgenic mice (Figure 2). Next, we examined the direct effect of LDIR on the changes of M1/M2 cytokines in cultured microglial BV-2 cells. Surprisingly, the mRNA and protein levels of M1 proinflammatory cytokines, such as TNF- α , IL-1 β , and IL-6, were significantly reduced and the mRNA and protein levels of M2 anti-inflammatory cytokines, such as TGF- α , TGF- β , and IL-10, were significantly increased in the LPS-treated microglia after the exposure of LDIR when compared to LPS-stimulated cells (Figure 3). Moreover, the LDIR treatment significantly increased expression of M2 phenotypic marker CD206 in LPS-treated microglia (Figure 4), suggesting that the interaction between LPS and LDIR therapy can switch the microglial phenotype from M1 to M2. Additionally, expression of TREM2 involved in microglial M1/M2 polarization was increased after the LDIR exposure in LPS-stimulated microglia (Figure 5). Taken together, it has been suggested that the LDIR treatment inhibits the cognitive deficit and A β deposition in AD by modulating the polarization of microglial phenotype and expression of TREM2 (Figure 6A).

Plasma levels of LPS in AD patients have been reported to be three times higher than in normal individuals [56]. Similar to A β , LPS is known to cause inflammation in the central nervous system [57]. LPS significantly contributes to the pathogenesis of AD and is well-established as a one of the risk factors for AD [5,9,10]. In addition, LPS-induced inflammation acts as an upstream of A β pathology by increasing A β production [5,7,8]. Moreover, LPS damages the blood brain barrier (BBB), allowing more LPS to enter the brain [58]. Furthermore, LPS interacts directly with microglia to induce acute inflammatory responses, and neurotoxic molecules from activated microglia are well known to cause the neurodegeneration [57,59–61]. Our LPS-treated results are inconsistent with previous studies showing that LPS-induced microglial phenotypic changes characterized by increase of M1 marker, and decrease of M2 marker [62–65]. Since various factors such as cell line, serotype, species, dose of LPS, and batch of LPS contents have affected the inflammatory reaction, we speculated that our results were not consistent with the previous studies. Although CD 86 and CD 206 were not significantly changed in this study (Figure 4), it is certain that LPS provoked an inflammatory response and affected the microglial phenotype changes. Notably, LPS has been reported to downregulate TREM2 expression through the NF- κ B pathway [66,67]. Surprisingly, in our study, LPS+LDIR or LDIR-induced upregulation of TREM2 was detected at the level of mRNA, and is related with inhibition of pro-inflammatory cytokines and consequently suppression of AD pathology [68]. Taken together, not only A β but also LPS can be identified as a critical factor that disrupts microglial phenotype-related homeostasis in AD [32]. Therefore, LPS is one of the inflammatory triggers in AD progression, indicating that LPS-mediated inflammation can directly contribute to pathogenesis of AD [69].

In AD, it has been shown that A β and tau result in a hyper-activated M1 phenotype of microglial cells, leading to detrimental brain damage concomitant with the expression of pro-inflammatory cytokines, such as TNF- α , IL-1 β , and IL-6. In contrast, the M2 phenotype of microglial cells can induce neuroprotective functions and restore the brain environment through the action of neurotrophic factors [70]. In addition, it has been known that, after exposure to LDIR, air-pouch mouse show the down-regulation of TNF- α and IL-1 β , which are the representative M1 cytokines, whereas the expression of anti-inflammatory M2 cytokine TGF β -1 was up-regulated in air-pouch mouse [71]. In the present study, we examined whether the phenotype of microglia cells could be changed by LDIR therapy through the detection of M1 and M2 cytokines in in vivo and in vitro models of AD. We found that the LDIR treatment down-regulated of M1 cytokines and up-regulated M2 cytokines in 5XFAD

mice or BV-2 cells activated by LPS (Figures 2 and 3). In order to confirm the phenotype change of microglia cells specifically, further study is needed to perform the double labeling of microglia cells and TNF- α and TGF- β . Taken together, these data indicate that LDIR therapy strongly modulates the release of M1 and M2 cytokines in the brain with AD.

TREM2 has been known to be a major regulator for microglial phenotype switching [32]. Heterozygous rare variants (R47H) of TREM2 in AD reduce the expression of TREM2 and cell surface transport function [24,72]. TREM2 deficiency in the AD animal models resulted in reduction of the number of microglia around the A β plaques and aggravation of the A β pathology [73–75]. In addition, microglia with decreased TREM2 levels predominantly exhibited the M1 phenotype and secreted neurotoxic cytokines [76]. In contrast, the secretion of pro-inflammatory cytokines by M1 polarization was reduced in TREM2-overexpressing mouse model [31]. Furthermore, increased expression of TREM2 resulted in both reduction of M1 microglia, which contribute to AD pathogenesis by inducing pro-inflammatory responses and neuronal damage [77], and increase of M2 microglia, which ameliorate AD pathology through release of anti-inflammatory cytokines and neurotropic factors [78]. In the BV-2 cell, knockdown of TREM2 expression increases M1 inflammatory responses and inhibits phenotype switching to M2, while overexpression of TREM2 promotes phenotype change to M2 and alleviated inflammation of M1 [22]. Interestingly, our results revealed that LDIR increased mRNA levels of TREM2 in LPS-treated BV-2 cells (Figure 5). Accordingly, it seems likely that the LDIR therapy might induce M1/M2 phenotype changes via increasing the expression of TREM2 in the microglia within AD brain (Figure 6B). However, it should be cautioned to interpret our results because the microglia polarization concept is controversial in the neuroscience field.

Radiation therapy (20 Gy/10 fractions) has been used for decades to treat extra-cranial amyloidosis, especially when the deposits cause airway obstructions in the trachea [79,80]. Recent studies have emerged that address the potential application of LDIR in treating AD caused by accumulation of misfolded proteins such as A β and tau [79]. Current therapies for AD only target specific proteins, such as A β or tau, and these clinical studies targeting for A β or tau have failed to improve the cognitive function of patients. However, LDIR not only targets pathogenic protein, such as A β , but also has an indirect effect that involves the phenotype shifting microglial cells. The data presented in this study suggest that LDIR therapy could effectively improve cognitive function in AD.

Although the mechanism underlying the effects of radiation therapy for AD has not yet been completely elucidated, previous reports and the results of the current study have suggested the possible therapeutic mechanisms mediated by LDIR exposure. Firstly, LDIR may cause neuroprotection via up-regulation of neurotrophic factors, such as TGF- β and IL-10, as reported in the present study. In addition, TGF- β has also been reported to be involved in cell growth and maintenance [81,82]. Additionally, we discovered that LDIR provokes microglia phenotype shifting from an M1 to M2 phenotype under LPS and AD treatment. Thus, increased phagocytosis mediated by M2 polarization can lead to an increase in clearance of abnormal proteins such as A β [83]. Secondly, LDIR up-regulates the expression of synaptophysin and intercellular adhesion molecules (CAM) [84,85], which enable synaptic plasticity and promote synaptogenesis. Enhancement of synaptogenesis can improve cognitive function [86]. Thirdly, LDIR up-regulates heat shock protein 70, a protein that has been reported to regulate misfolded protein aggregation and may reduce the toxicity of A β [87,88]. Finally, LDIR induces up-regulation of vascular endothelial growth factors (VEGF), which enhances the patency of the dysfunctional lymphatic pathway triggered by AD pathology and is subsequently involved in the drainage of A β [89–93].

Based on the abovementioned mechanisms, in August 2019, our research team initiated a study investigating the effect of 2 regimens of LDIR therapy (9 Gy/5 fraction and 5.4 Gy/3 fraction) on A β plaque formation and cognitive function in patients with early or moderate AD. We started a randomized prospective phase II clinical trial to assess if LDIR therapy could inhibit cognitive decline in AD (NCT 04203121). Currently, approximately six clinical trials have been conducted, not only in

South Korea, but also in the US and Europe and are expected to yield effective clinical outcomes within a few years.

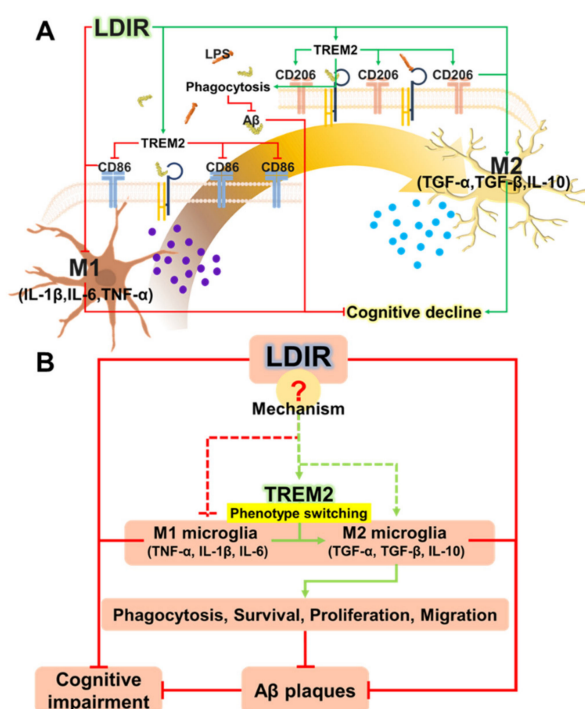


Figure 6. (A) Schematic drawing of the modulatory effects of LDIR exposure on shifting microglial phenotypes. (B) Proposed mechanisms for how LDIR treatment is able to reduce A β accumulation and cognitive decline.

4. Materials and Methods

4.1. Reagents

LPS from *Escherichia coli*, serotype 026: B6, was purchased from the Sigma-Aldrich Chemical Company (St. Louis, MO, USA). Thioflavin S was purchased from Sigma-Aldrich Chemical Company (T1892-25G).

4.2. Animals

The male heterozygous 5XFAD transgenic mice (C57BL/6-SJL background; 6-month-old; obtained from Jun biotech, Inc, Republic of Korea) were used. The 5XFAD mice was identified by genotyping. Wild-type (WT) littermates of 5XFAD mice were used controls. Mice were sacrificed 8 weeks after LDIR treatment. All experiments detailed herein complied with the regulations specified by Kyung Hee University Guidelines for Laboratory Animal Care and Use. This animal research was approved by committee of Kyung Hee University Hospital in Gangdong (project identification code: KHNMC AP 2017-003, date: 21 February 2017).

4.3. Radiation Exposure

X-ray irradiating system (LEP-300, Auracare[®], Gyeonggi-do, Korea) and X-ray tube (320 kVp, 15 mA, Varian Medical Systems, Inc., USA) were used for all irradiation procedures, which were performed at room temperature. For the in vivo experiments, mice were anesthetized with 2.5 mg/kg Zoletil, placed in an immobilizer, and exposed to a total radiation dose of 10 Gy/5 fractions. Cells were cultured in a 60 × 15 mm dish. Immediately before irradiation exposure, the culture dish was filled with media and all air gaps were eliminated. The cells were then exposed to a 50, 100, 200, 380,

or 525 cGy/fraction of radiation (Figure S1). Lead shields protected the sham-treated cells and mice during exposure of the radiation.

4.4. Memory Test

The spatial learning and memory of mice were evaluated using the Morris water maze task, as previously described [94]. The experimental procedures were recorded on videotape.

4.5. Confocal Microscopy

Brain tissue blocks were cryo-sectioned at a thickness of 7 μm . For A β histology staining, the sections were incubated in 0.5% thioflavin-S (50% in ethanol) for 10 min, then washed with 50% ethanol, and finally with PBS. Fluorescence signal was assessed using the Zeiss LSM 700 laser confocal microscopy system.

4.6. Real-Time Quantitative Reverse Transcription Polymerase Chain Reaction

Total RNA was extracted from BV-2 cells or brain samples of mice using an RNA purification kit (Gene All, Seoul, Republic of Korea) according to the manufacturer's protocols. Complementary DNA (cDNA) was generated using Revert Aid First Strand cDNA Synthesis Kit (Thermo Scientific, Waltham, MA, USA) and was subjected to qRT-PCR analysis using SYBR Green PCR master mix (Thermo Scientific, Waltham, MA, USA). The gene-specific primer sequences for M1/M2 markers and GAPDH are listed in Table S1. The relative expression of each gene was calculated using the $\Delta\Delta\text{Cq}$ method with GAPDH. For quantification, the quantification cycle (Cq) values were normalized with GAPDH Cq and analyzed with the Comparative CT Method $2^{-\Delta\Delta\text{Cq}}$ method, as previously described [95].

4.7. Enzyme-Linked Immunosorbent Assay

The effect of LDIR exposure on the protein levels of M1 (TNF- α , IL-1 β , and IL-6) and M2 (TGF- α , TGF- β , and IL-10) cytokines was analyzed by ELISA. Cell-free culture supernatants were collected and 50 μL of undiluted cultured media per well was analyzed for M1 or M2 cytokines by a specific ELISA kit (mouse inflammatory cytokine multianalyte ELISA array kit; Qiagen) according to the manufacturer's recommendations.

4.8. BV-2 Cell Culture

The murine microglia cell line BV-2 were maintained at 37 $^{\circ}\text{C}$ and 5% CO_2 in Dulbecco's modified Eagle's medium (DMEM) supplemented with 2 mM glutamine, 100 $\mu\text{g}/\text{mL}$ streptomycin, 100 units/mL penicillin, and 10% heat-inactivated fetal bovine serum (FBS).

4.9. Cell Viability

The Cell counting kit-8 (CCK-8) assay was used to determine cell viability after treatment of LPS and LDIR. CCK-8 assay was conducted following the manufacturer's protocol (Dojindo Molecular Technologies, Kumamoto, Japan). Emax Plus Microplate Reader (Molecular Devices Emax, CA, USA) was used to measure the absorbance of each well at 540 nm.

4.10. Immunoblotting

The BV-2 cells were homogenized with RIPA buffer and protease inhibitors (Thermo Scientific). Equal amounts of protein (40 $\mu\text{g}/\text{lane}$) were loaded to gradient (4 to 15%) concentrations of polyacrylamide SDS-PAGE (Smobio, Hsinchu City, Taiwan) and transferred to polyvinylidene difluoride (PVDF) membranes (Millipore, Billerica, MA) using an electro-transfer system (Bio-Rad, Hercules, CA). The membranes were blocked with 5% nonfat milk and probed with the following primary antibodies for 16 h at 4 $^{\circ}\text{C}$: rabbit polyclonal anti-CD206 (1:1,000; Abbkine, Wuhan, China),

goat polyclonal TREM2 (1:1,000, ThermoFisher Scientific), and mouse monoclonal β -actin (1:5,000; Abbkine). The membranes were incubated with the appropriate secondary antibodies (Bethyl, Inc., Montgomery, TX, USA) conjugated to horseradish peroxidase (HRP) for 1 h at room temperature. Bound antibodies were visualized with D-Plus ECL Pico System (Dongin LS, Republic of Korea) and a G: Box Chemiluminescence & Fluorescence system (Syngene, Frederick, MD, USA).

4.11. Statistics

Data are presented as means \pm SD. Paired samples' statistics using the student's *t*-test was conducted for analysis between sham-exposed and LDIR-exposed groups. For escape latency, repeated measure two-way analysis of variance (ANOVA) was used. The other analysis performed using the one-way ANOVA followed by Fisher's LSD post-hoc test for comparisons among the three groups. Asterisks indicate significant differences, as noted in the figure legends.

5. Conclusions

For the first time, we studied the effects of LDIR on polarization of microglia using both in vitro and in vivo models. LDIR not only affected the microglia phenotype shifting, but also clears amyloid plaques, resulting in inhibition of cognitive decline in AD. In future studies, we aim to focus on elucidating the mechanism by which LDIR affects these changes (Figure 6B), as well as identifying the optimal LDIR treatment regimen for diverse neurodegenerative diseases with a specific focus on AD.

Supplementary Materials: Supplementary materials can be found at <http://www.mdpi.com/1422-0067/21/12/4532/s1>.

Author Contributions: Conceptualization, M.M., and W.K.C.; methodology, S.K., H.C., and H.N.M.; software, S.K. and Y.N.; validation, M.J.C., and J.K.L.; formal analysis, S.K., H.C., Y.N., S.J.S., and Y.H.P.; investigation, H.N.M., H.Y.R., and G.-H.J.; resources, H.C., W.K.C., and M.M.; data curation, Y.K., Y.J.L., and M.K.; writing—original draft preparation, S.K.; writing—review and editing, H.C., M.M., and W.K.C.; visualization, S.K. and H.C.; supervision, M.M., and W.K.C.; project administration, W.K.C. and M.M.; funding acquisition, W.K.C. and M.M. All authors have read and agreed to the published version of the manuscript.

Funding: This study was supported by Ministry of SME and Startups Project Number: S2668252, the National Research Foundation of Korea (NRF) grant funded by the Korea government (MSIT) (NRF-2016R1D1A1B03935770 to W.K.C.), and Basic Science Research Program of the National Research Foundation of Korea (NRF), which is funded by the Ministry of Science, ICT & Future Planning (NRF-2018R1D1A3B07041059 to M.M.) and by the Cooperative Research Program for Agriculture Science and Technology Development (Project No. PJ01319901 and PJ01428603 to M.M.), Rural Development Administration, Republic of Korea.

Conflicts of Interest: The authors declare no conflicts of interest.

Abbreviations

AD	Alzheimer's disease
ANOVA	one-way analysis of variance
A β	amyloid- β
BBB	blood brain barrier
CAM	intercellular adhesion molecule
CCK-8	Cell counting kit-8
DMEM	Dulbecco's Modified Eagle Medium
IL-1 β	interleukin-1 beta
INF- γ	interferon-gamma
LDIR	Low-dose ionizing radiation
LPS	lipopolysaccharides
R47H	Heterozygous rare variants
TNF- α	tumor necrosis factor alpha
TREM2	triggering receptor expressed on myeloid cells 2
VEGF	vascular endothelial growth factors
WT	Wild-type

References

1. Lu, Q.; Powles, R.L.; Abdallah, S.; Ou, D.; Wang, Q.; Hu, Y.; Lu, Y.; Liu, W.; Li, B.; Mukherjee, S.; et al. Systematic tissue-specific functional annotation of the human genome highlights immune-related DNA elements for late-onset Alzheimer's disease. *Lancet* **2016**, *388*, 078865. [[CrossRef](#)]
2. Querfurth, H.W.; LaFerla, F.M. Alzheimer's disease. *N. Engl. J. Med.* **2010**, *362*, 329–344. [[CrossRef](#)]
3. Bolos, M.; Úbeda-Portugués, J.R.P.; Avila, J. Alzheimer's disease as an inflammatory disease. *Biomol. Concepts* **2017**, *8*, 37–43. [[CrossRef](#)] [[PubMed](#)]
4. Calsolaro, V.; Edison, P. Neuroinflammation in Alzheimer's disease: Current evidence and future directions. *Alzheimer's Dement.* **2016**, *12*, 719–732. [[CrossRef](#)] [[PubMed](#)]
5. Lee, J.W.; Lee, Y.K.; Yuk, D.Y.; Choi, D.-Y.; Han, S.-B.; Oh, K.-W.; Hong, J.T. Neuro-inflammation induced by lipopolysaccharide causes cognitive impairment through enhancement of beta-amyloid generation. *J. Neuroinflamm.* **2008**, *5*, 37. [[CrossRef](#)] [[PubMed](#)]
6. Rajendran, L.; Paolicelli, R.C. Microglia-Mediated Synapse Loss in Alzheimer's Disease. *J. Neurosci.* **2018**, *38*, 2911–2919. [[CrossRef](#)]
7. Sheng, J.G.; Bora, S.H.; Xu, G.; Borchelt, D.R.; Price, D.L.; Koliatsos, V.E. Lipopolysaccharide-induced-neuroinflammation increases intracellular accumulation of amyloid precursor protein and amyloid beta peptide in APP^{swe} transgenic mice. *Neurobiol. Dis.* **2003**, *14*, 133–145. [[CrossRef](#)]
8. Hauss-Wegrzyniak, B.; Wenk, G. Beta-amyloid deposition in the brains of rats chronically infused with thiorphan or lipopolysaccharide: The role of ascorbic acid in the vehicle. *Neurosci. Lett.* **2002**, *322*, 75–78. [[CrossRef](#)]
9. Pretorius, E.; Bester, J.; Kell, D.B. A Bacterial Component to Alzheimer's-Type Dementia Seen via a Systems Biology Approach that Links Iron Dysregulation and Inflammagen Shedding to Disease. *J. Alzheimer's Dis.* **2016**, *53*, 1237–1256. [[CrossRef](#)]
10. Lee, Y.-J.; Choi, N.-Y.; Yun, Y.-P.; Han, S.-B.; Oh, K.-W.; Hong, J.T. Epigallocatechin-3-gallate prevents systemic inflammation-induced memory deficiency and amyloidogenesis via its anti-neuroinflammatory properties. *J. Nutr. Biochem.* **2013**, *24*, 298–310. [[CrossRef](#)]
11. Block, M.L.; Zecca, L.; Hong, J.-S. Microglia-mediated neurotoxicity: Uncovering the molecular mechanisms. *Nat. Rev. Neurosci.* **2007**, *8*, 57–69. [[CrossRef](#)] [[PubMed](#)]
12. Chen, Z.; Trapp, B.D. Microglia and neuroprotection. *J. Neurochem.* **2015**, *136*, 10–17. [[CrossRef](#)] [[PubMed](#)]
13. Davis, B.M.; Salinas-Navarro, M.; Cordeiro, M.F.; Moons, L.; De Groef, L. Characterizing microglia activation: A spatial statistics approach to maximize information extraction. *Sci. Rep.* **2017**, *7*. [[CrossRef](#)]
14. Zhang, L.; Zhang, J.; You, Z. Switching of the Microglial Activation Phenotype Is a Possible Treatment for Depression Disorder. *Front. Cell. Neurosci.* **2018**, *12*, 306. [[CrossRef](#)] [[PubMed](#)]
15. Nakagawa, Y.; Chiba, K. Role of microglial m1/m2 polarization in relapse and remission of psychiatric disorders and diseases. *Pharmaceuticals (Basel)* **2014**, *7*, 1028–1048. [[CrossRef](#)] [[PubMed](#)]
16. Pathipati, P.; Müller, S.; Jiang, X.; Ferriero, N. Phenotype and Secretory Responses to Oxidative Stress in Microglia. *Dev. Neurosci.* **2013**, *35*, 241–254. [[CrossRef](#)]
17. Boche, D.; Perry, V.H.; Nicoll, J.A.R. Review: Activation patterns of microglia and their identification in the human brain. *Neuropathol. Appl. Neurobiol.* **2013**, *39*, 3–18. [[CrossRef](#)]
18. Wynn, T.; Vannella, K.M. Macrophages in Tissue Repair, Regeneration, and Fibrosis. *Immunity* **2016**, *44*, 450–462. [[CrossRef](#)]
19. Varnum, M.M.; Ikezu, T. The classification of microglial activation phenotypes on neurodegeneration and regeneration in Alzheimer's disease brain. *Arch. Immunol. et Ther. Exp.* **2012**, *60*, 251–266. [[CrossRef](#)]
20. Liu, C.-Y.; Wang, X.; Liu, C.; Zhang, H.-L. Pharmacological Targeting of Microglial Activation: New Therapeutic Approach. *Front. Cell. Neurosci.* **2019**, *13*, 514. [[CrossRef](#)]
21. Carmona, S.; Zahs, K.; Wu, E.; Dakin, K.; Bras, J.; Guerreiro, R. The role of TREM2 in Alzheimer's disease and other neurodegenerative disorders. *Lancet Neurol.* **2018**, *17*, 721–730. [[CrossRef](#)]
22. Zhang, Y.; Feng, S.; Nie, K.; Li, Y.; Gao, Y.; Gan, R.; Wang, L.; Li, B.; Sun, X.; Wang, L.; et al. TREM2 modulates microglia phenotypes in the neuroinflammation of Parkinson's disease. *Biochem. Biophys. Res. Commun.* **2018**, *499*, 797–802. [[CrossRef](#)] [[PubMed](#)]

23. Fan, Y.; Ma, Y.; Huang, W.; Cheng, X.; Gao, N.; Li, G.; Tian, S. Up-regulation of TREM2 accelerates the reduction of amyloid deposits and promotes neuronal regeneration in the hippocampus of amyloid beta1-42 injected mice. *J. Chem. Neuroanat.* **2019**, *97*, 71–79. [[CrossRef](#)] [[PubMed](#)]
24. Sarlus, H.; Heneka, M.T. Microglia in Alzheimer's disease. *J. Clin. Investig.* **2017**, *127*, 3240–3249. [[CrossRef](#)]
25. Zheng, H.; Cheng, B.; Li, Y.; Li, X.; Chen, X.; Zhang, Y.-W. TREM2 in Alzheimer's Disease: Microglial Survival and Energy Metabolism. *Front. Aging Neurosci.* **2018**, *10*, 395. [[CrossRef](#)]
26. Bouchon, A.; Hernández-Munain, C.; Cella, M.; Colonna, M. A Dap12-Mediated Pathway Regulates Expression of Cc Chemokine Receptor 7 and Maturation of Human Dendritic Cells. *J. Exp. Med.* **2001**, *194*, 1111–1122. [[CrossRef](#)]
27. Bhattacharjee, S.; Zhao, Y.; Dua, P.; Rogaev, E.I.; Lukiw, W.J. microRNA-34a-Mediated Down-Regulation of the Microglial-Enriched Triggering Receptor and Phagocytosis-Sensor TREM2 in Age-Related Macular Degeneration. *PLoS ONE* **2016**, *11*, e0150211. [[CrossRef](#)]
28. Zheng, H.; Liu, C.-C.; Atagi, Y.; Chen, X.-F.; Jia, L.; Yang, L.; He, W.; Zhang, X.; Kang, S.S.; Rosenberry, T.L.; et al. Opposing roles of the triggering receptor expressed on myeloid cells 2 and triggering receptor expressed on myeloid cells-like transcript 2 in microglia activation. *Neurobiol. Aging* **2016**, *42*, 132–141. [[CrossRef](#)]
29. Takahashi, K.; Rochford, C.D.; Neumann, H. Clearance of apoptotic neurons without inflammation by microglial triggering receptor expressed on myeloid cells-2. *J. Exp. Med.* **2005**, *201*, 647–657. [[CrossRef](#)]
30. Lee, C.D.; Daggett, A.; Gu, X.; Jiang, L.-L.; Langfelder, P.; Li, X.; Wang, N.; Zhao, Y.; Park, C.S.; Cooper, Y.; et al. Elevated TREM2 Gene Dosage Reprograms Microglia Responsivity and Ameliorates Pathological Phenotypes in Alzheimer's Disease Models. *Neuron* **2018**, *97*, 1032–1048.e5. [[CrossRef](#)]
31. Jiang, T.; Zhang, Y.; Chen, Q.; Gao, Q.; Zhu, X.-C.; Zhou, J.; Shi, J.-Q.; Lu, H.; Tan, L.; Yu, J. TREM2 modifies microglial phenotype and provides neuroprotection in P301S tau transgenic mice. *Neuropharmacology* **2016**, *105*, 196–206. [[CrossRef](#)] [[PubMed](#)]
32. Krasemann, S.; Madore, C.; Cialic, R.; Baufeld, C.; Calcagno, N.; El Fatimy, R.; Beckers, L.; O'Loughlin, E.; Xu, Y.; Fanek, Z.; et al. The TREM2-APOE Pathway Drives the Transcriptional Phenotype of Dysfunctional Microglia in Neurodegenerative Diseases. *Immunity* **2017**, *47*, 566–581.e9. [[CrossRef](#)] [[PubMed](#)]
33. Gervois, P.; Lambrechts, I. The Emerging Role of Triggering Receptor Expressed on Myeloid Cells 2 as a Target for Immunomodulation in Ischemic Stroke. *Front. Immunol.* **2019**, *10*, 1668. [[CrossRef](#)] [[PubMed](#)]
34. Keren-Shaul, H.; Spinrad, A.; Weiner, A.; Matcovitch-Natan, O.; Dvir-Szternfeld, R.; Ulland, T.K.; David, E.; Baruch, K.; Lara-Astaiso, D.; Toth, B.; et al. A Unique Microglia Type Associated with Restricting Development of Alzheimer's Disease. *Cell* **2017**, *169*, 1276–1290.e17. [[CrossRef](#)]
35. Monje, M.L.; Mizumatsu, S.; Fike, J.R.; Palmer, T.D. Irradiation induces neural precursor-cell dysfunction. *Nat. Med.* **2002**, *8*, 955–962. [[CrossRef](#)]
36. Chakraborti, A.; Allen, A.; Allen, B.; Rosi, S.; Fike, J.R. Cranial Irradiation Alters Dendritic Spine Density and Morphology in the Hippocampus. *PLoS ONE* **2012**, *7*, e40844. [[CrossRef](#)]
37. Shirai, K.; Mizui, T.; Suzuki, Y.; Okamoto, M.; Hanamura, K.; Yoshida, Y.; Hino, M.; Noda, S.-E.; Al-Jahdari, W.S.; Chakravarti, A.; et al. X Irradiation Changes Dendritic Spine Morphology and Density through Reduction of Cytoskeletal Proteins in Mature Neurons. *Radiat. Res.* **2013**, *179*, 630–636. [[CrossRef](#)]
38. Wilson, G.D.; Marples, B. A New Use for an Old Treatment: Radiation Therapy and Alzheimer's Disease. *Radiat. Res.* **2016**, *185*, 443–448. [[CrossRef](#)]
39. Michael, D.B.; Wilson, G.D.; Hanna, A.; Wilson, T.; Martinez, A.A.; Chinnaiyan, P.; Maddens, M.E.; Fontanesi, J. Radiation therapy for the treatment of Alzheimer's disease. *Neurol. Neurosurg.* **2019**, *2*, 1. [[CrossRef](#)]
40. Ceyzériat, K.; Tournier, B.B.; Millet, P.; Frisoni, G.B.; Garibotto, V.; Zilli, T. Low-Dose Radiation Therapy: A New Treatment Strategy for Alzheimer's Disease? *J. Alzheimer's Dis.* **2020**, *74*, 411–419. [[CrossRef](#)]
41. Kim, S.; Nam, Y.; Kim, C.; Lee, H.; Hong, S.; Kim, H.S.; Shin, S.J.; Park, Y.H.; Mai, H.N.; Oh, S.-M.; et al. Neuroprotective and Anti-Inflammatory Effects of Low-Moderate Dose Ionizing Radiation in Models of Alzheimer's Disease. *Int. J. Mol. Sci.* **2020**, *21*, 3678. [[CrossRef](#)] [[PubMed](#)]
42. Cuttler, J.S.W.J.M.; Moore, E.R.; Hosfeld, V.D.; Nadolski, D.L. Treatment of Alzheimer Disease With CT Scans. *Dose Response* **2016**, *14*, 1559325816640073. [[CrossRef](#)] [[PubMed](#)]

43. Liu, B.; Hinshaw, R.G.; Le, K.X.; Park, M.-A.; Wang, S.; Belanger, A.P.; Dubey, S.; Frost, J.L.; Shi, Q.; Holton, P.; et al. Space-like ⁵⁶Fe irradiation manifests mild, early sex-specific behavioral and neuropathological changes in wildtype and Alzheimer's-like transgenic mice. *Sci. Rep.* **2019**, *9*, 12118. [[CrossRef](#)]
44. Wei, L.-C.; Ding, Y.-X.; Liu, Y.; Duan, L.; Bai, Y.; Shi, M.; Chen, L.-W. Low-dose radiation stimulates Wnt/ β -catenin signaling, neural stem cell proliferation and neurogenesis of the mouse hippocampus in vitro and in vivo. *Curr. Alzheimer Res.* **2012**, *9*, 278–289. [[CrossRef](#)] [[PubMed](#)]
45. Marples, B.; McGee, M.; Callan, S.; Bowen, S.; Thibodeau, B.J.; Michael, D.B.; Wilson, G.D.; Maddens, M.E.; Fontanesi, J.; Martinez, A.A. Cranial irradiation significantly reduces beta amyloid plaques in the brain and improves cognition in a murine model of Alzheimer's Disease (AD). *Radiother. Oncol.* **2016**, *118*, 579–580. [[CrossRef](#)] [[PubMed](#)]
46. Kempf, S.J.; Janik, D.; Barjaktarovic, Z.; Braga-Tanaka, I., 3rd; Tanaka, S.; Neff, F.; Saran, A.; Larsen, M.R.; Tapio, S. Chronic low-dose-rate ionising radiation affects the hippocampal phosphoproteome in the ApoE-/Alzheimer's mouse model. *Oncotarget* **2016**, *7*(44), 71817–71832. [[CrossRef](#)] [[PubMed](#)]
47. Otani, A.; Kojima, H.; Guo, C.; Oishi, A.; Yoshimura, N. Low-Dose-Rate, Low-Dose Irradiation Delays Neurodegeneration in a Model of Retinitis Pigmentosa. *Am. J. Pathol.* **2012**, *180*, 328–336. [[CrossRef](#)]
48. Bachstetter, A.D.; Norris, C.M.; Sompol, P.; Wilcock, D.M.; Goulding, D.; Neltner, J.H.; Clair, D.S.; Watterson, D.M.; Van Eldik, L.J. Early stage drug treatment that normalizes proinflammatory cytokine production attenuates synaptic dysfunction in a mouse model that exhibits age-dependent progression of Alzheimer's disease-related pathology. *J. Neurosci.* **2012**, *32*, 10201–10210. [[CrossRef](#)]
49. Tang, Y.; Le, W. Differential Roles of M1 and M2 Microglia in Neurodegenerative Diseases. *Mol. Neurobiol.* **2015**, *53*, 1181–1194. [[CrossRef](#)]
50. Kacimi, R.; Giffard, R.G.; Yenari, M.A. Endotoxin-activated microglia injure brain derived endothelial cells via NF-kappaB, JAK-STAT and JNK stress kinase pathways. *J. Inflamm. (Lond.)* **2011**, *8*. [[CrossRef](#)]
51. Park, B.-K.; Kim, Y.H.; Kim, Y.R.; Choi, J.J.; Yang, C.; Jang, I.S.; Lee, M.Y. Antineuroinflammatory and Neuroprotective Effects of Gyejibokryeong-Hwan in Lipopolysaccharide-Stimulated BV2 Microglia. *Evid. Based Complement. Altern. Med.* **2019**, *2019*, 7585896. [[CrossRef](#)] [[PubMed](#)]
52. Lively, S.; Schlichter, L.C. The microglial activation state regulates migration and roles of matrix-dissolving enzymes for invasion. *J. Neuroinflamm.* **2013**, *10*, 75. [[CrossRef](#)] [[PubMed](#)]
53. Zhang, F.; Zhong, R.; Li, S.; Fu, Z.; Cheng, C.; Cai, H.; Le, W. Acute Hypoxia Induced an Imbalanced M1/M2 Activation of Microglia through NF-kappaB Signaling in Alzheimer's Disease Mice and Wild-Type Littermates. *Front. Aging Neurosci.* **2017**, *9*, 282. [[CrossRef](#)] [[PubMed](#)]
54. Peng, H.; Nickell, C.R.G.; Chen, K.Y.; McClain, J.A.; Nixon, K. Increased expression of M1 and M2 phenotypic markers in isolated microglia after four-day binge alcohol exposure in male rats. *Alcohol* **2017**, *62*, 29–40. [[CrossRef](#)] [[PubMed](#)]
55. Erkenstam, N.H.; Smith, P.L.P.; Fleiss, B.; Nair, S.; Svedin, P.; Wang, W.; Boström, M.; Gressens, P.; Hagberg, H.; Brown, K.L.; et al. Temporal Characterization of Microglia/Macrophage Phenotypes in a Mouse Model of Neonatal Hypoxic-Ischemic Brain Injury. *Front. Cell. Neurosci.* **2016**, *10*, 176. [[CrossRef](#)]
56. Zhang, R.; Miller, R.G.; Gascon, R.; Champion, S.; Katz, J.; Lancero, M.; Narvaez, A.; Honrada, R.; Ruvalcaba, D.; McGrath, M.S. Circulating endotoxin and systemic immune activation in sporadic amyotrophic lateral sclerosis (sALS). *J. Neuroimmunol.* **2008**, *206*, 121–124. [[CrossRef](#)]
57. Lull, M.E.; Block, M.L. Microglial activation and chronic neurodegeneration. *Neurotherapeutics* **2010**, *7*, 354–365. [[CrossRef](#)]
58. Varatharaj, A.; Galea, I. The blood-brain barrier in systemic inflammation. *Brain Behav. Immun.* **2017**, *60*, 1–12. [[CrossRef](#)]
59. Gu, C.; Hu, Q.; Wu, J.; Mu, C.; Ren, H.-G.; Liu, C.-F.; Wang, G. P7C3 Inhibits LPS-Induced Microglial Activation to Protect Dopaminergic Neurons Against Inflammatory Factor-Induced Cell Death in vitro and in vivo. *Front. Cell. Neurosci.* **2018**, *12*, 400. [[CrossRef](#)]
60. Katafuchi, T.; Ifuku, M.; Mawatari, S.; Noda, M.; Miake, K.; Sugiyama, M.; Fujino, T. Effects of plasmalogens on systemic lipopolysaccharide-induced glial activation and beta-amyloid accumulation in adult mice. *Ann. N. Y. Acad. Sci.* **2012**, *1262*, 85–92. [[CrossRef](#)]

61. Sorrenti, V.; Contarini, G.; Sut, S.; Dall'Acqua, S.; Confortin, F.; Pagetta, A.; Giusti, P.; Zusso, M. Curcumin Prevents Acute Neuroinflammation and Long-Term Memory Impairment Induced by Systemic Lipopolysaccharide in Mice. *Front. Pharmacol.* **2018**, *9*, 183. [[CrossRef](#)] [[PubMed](#)]
62. Chhor, V.; Le Charpentier, T.; Lebon, S.; Oré, M.-V.; Celador, I.L.; Josserand, J.; Degos, V.; Jacotot, E.; Hagberg, H.; Sävman, K.; et al. Characterization of phenotype markers and neuronotoxic potential of polarised primary microglia in vitro. *Brain Behav. Immun.* **2013**, *32*, 70–85. [[CrossRef](#)] [[PubMed](#)]
63. Shi, H.; Wang, X.L.; Quan, H.F.; Yan, L.; Pei, X.Y.; Wang, R.; Peng, X.D. Effects of Betaine on LPS-Stimulated Activation of Microglial M1/M2 Phenotypes by Suppressing TLR4/NF-kappaB Pathways in N9 Cells. *Molecules* **2019**, *24*, 367. [[CrossRef](#)]
64. Vay, S.U.; Flitsch, L.J.; Rabenstein, M.; Rogall, R.; Blaschke, S.; Kleinhaus, J.; Reinert, N.; Bach, A.; Fink, G.R.; Schroeter, M.; et al. The plasticity of primary microglia and their multifaceted effects on endogenous neural stem cells in vitro and in vivo. *J. Neuroinflamm.* **2018**, *15*, 226. [[CrossRef](#)]
65. Cianciulli, A.; Salvatore, R.; Porro, C.; Trotta, T.; Panaro, M.A. Folic Acid Is Able to Polarize the Inflammatory Response in LPS Activated Microglia by Regulating Multiple Signaling Pathways. *Mediat. Inflamm.* **2016**, *2016*, 1–10. [[CrossRef](#)]
66. Neumann, H.; Daly, M.J. Variant TREM2 as risk factor for Alzheimer's disease. *N. Engl. J. Med.* **2012**, *368*, 182–184. [[CrossRef](#)]
67. Owens, R.; Grabert, K.; Davies, C.L.; Alfieri, A.; Antel, J.P.; Healy, L.M.; McColl, B.W. Divergent Neuroinflammatory Regulation of Microglial TREM Expression and Involvement of NF-kappaB. *Front. Cell Neurosci.* **2017**, *11*, 56. [[CrossRef](#)]
68. Jiang, T.; Tan, L.; Zhu, X.-C.; Zhang, Q.-Q.; Cao, L.; Tan, M.-S.; Gu, L.-Z.; Wang, H.-F.; Ding, Z.-Z.; Zhang, Y.-D.; et al. Upregulation of TREM2 Ameliorates Neuropathology and Rescues Spatial Cognitive Impairment in a Transgenic Mouse Model of Alzheimer's Disease. *Neuropsychopharmacology* **2014**, *39*, 2949–2962. [[CrossRef](#)]
69. Zhan, X.; Stamova, B.; Sharp, F.R. Lipopolysaccharide Associates with Amyloid Plaques, Neurons and Oligodendrocytes in Alzheimer's Disease Brain: A Review. *Front. Aging Neurosci.* **2018**, *10*, 42. [[CrossRef](#)]
70. Hsieh, Y.-C.; Guo, C.; Yalamanchili, H.K.; Abreha, M.; Al-Ouran, R.; Li, Y.; Dammer, E.B.; Lah, J.J.; Levey, A.I.; Bennett, D.A.; et al. Tau-Mediated Disruption of the Spliceosome Triggers Cryptic RNA-Splicing and Neurodegeneration in Alzheimer's Disease. *SSRN Electron. J.* **2019**, *29*(2), 301. [[CrossRef](#)]
71. Schaeue, D.; Jahns, J.; Hildebrandt, G.; Trott, K.-R. Radiation treatment of acute inflammation in mice. *Int. J. Radiat. Biol.* **2005**, *81*, 657–667. [[CrossRef](#)] [[PubMed](#)]
72. Guerreiro, R.; Wojtas, A.; Bras, J.; Carrasquillo, M.; Rogaeva, E.; Majounie, E.; Cruchaga, C.; Sassi, C.; Kauwe, J.S.; Younkin, S.; et al. TREM2 variants in Alzheimer's disease. *N. Engl. J. Med.* **2012**, *368*, 117–127. [[CrossRef](#)] [[PubMed](#)]
73. Colonna, M.; Butovsky, O. Microglia Function in the Central Nervous System During Health and Neurodegeneration. *Annu. Rev. Immunol.* **2017**, *35*, 441–468. [[CrossRef](#)] [[PubMed](#)]
74. Wang, Y.; Cella, M.; Mallinson, K.; Ulrich, J.D.; Young, K.L.; Robinette, M.L.; Gilfillan, S.; Krishnan, G.M.; Sudhakar, S.; Zinselmeyer, B.; et al. TREM2 lipid sensing sustains the microglial response in an Alzheimer's disease model. *Cell* **2015**, *160*, 1061–1071. [[CrossRef](#)] [[PubMed](#)]
75. Jay, T.; Miller, C.M.; Cheng-Hathaway, P.; Graham, L.C.; BeMiller, S.; Broihier, M.L.; Xu, G.; Margevicius, D.; Karlo, J.C.; Sousa, G.L.; et al. TREM2 deficiency eliminates TREM2+ inflammatory macrophages and ameliorates pathology in Alzheimer's disease mouse models. *J. Exp. Med.* **2015**, *212*, 287–295. [[CrossRef](#)] [[PubMed](#)]
76. Jiang, T.; Yu, J.; Zhu, X.-C.; Tan, L. TREM2 in Alzheimer's disease. *Mol. Neurobiol.* **2013**, *48*, 180–185. [[CrossRef](#)]
77. Shen, Z.; Bao, X.; Wang, R. Clinical PET Imaging of Microglial Activation: Implications for Microglial Therapeutics in Alzheimer's Disease. *Front. Aging Neurosci.* **2018**, *10*, 314. [[CrossRef](#)]
78. Jin, X.; Liu, M.-Y.; Zhang, D.-F.; Zhong, X.; Du, K.; Qian, P.; Gao, H.; Wei, Q. Natural products as a potential modulator of microglial polarization in neurodegenerative diseases. *Pharmacol. Res.* **2019**, *145*, 104253. [[CrossRef](#)]
79. Marples, B.; McGee, M.; Callan, S.; Bowen, S.; Thibodeau, B.J.; Michael, D.B.; Wilson, G.D.; Maddens, M.E.; Fontanesi, J.; Martinez, A.A.; et al. Cranial irradiation significantly reduces beta amyloid plaques in the brain and improves cognition in a murine model of Alzheimer's Disease (AD). *Radiother. Oncol.* **2016**, *118*, 43–51. [[CrossRef](#)]

80. Kurrus, J.A.; Hayes, J.K.; Hoidal, J.R.; Menendez, M.M.; Elstad, M.R. Radiation therapy for tracheobronchial amyloidosis. *Chest* **1998**, *114*, 1489–1492. [[CrossRef](#)]
81. Kang, J.H.; Jung, M.Y.; Yin, X.; Andrianifahanana, M.; Hernandez, D.M.; Leof, E.B. Cell-penetrating peptides selectively targeting SMAD3 inhibit profibrotic TGF-beta signaling. *J. Clin. Investig.* **2017**, *127*, 2541–2554. [[CrossRef](#)] [[PubMed](#)]
82. Butovsky, O.; Jedrychowski, M.P.; Moore, C.S.; Cialic, R.; Lanser, A.J.; Gabriely, G.; Koeglsperger, T.; Dake, B.; Wu, P.M.; Doykan, C.E.; et al. Identification of a unique TGF-beta-dependent molecular and functional signature in microglia. *Nat. Neurosci.* **2014**, *17*, 131–143. [[CrossRef](#)] [[PubMed](#)]
83. Sokolowski, J.D.; Mandell, J.W. Phagocytic Clearance in Neurodegeneration. *Am. J. Pathol.* **2011**, *178*, 1416–1428. [[CrossRef](#)] [[PubMed](#)]
84. Moravan, M.J.; Olschowka, J.A.; Williams, J.P.; O'Banion, M.K. Cranial irradiation leads to acute and persistent neuroinflammation with delayed increases in T-cell infiltration and CD11c expression in C57BL/6 mouse brain. *Radiat. Res.* **2011**, *176*, 459–473. [[CrossRef](#)]
85. Olschowka, J.A.; Kyrkanides, S.; Harvey, B.K.; O'Banion, M.K.; Williams, J.P.; Rubin, P.; Hansen, J.T. ICAM-1 Induction in the Mouse CNS Following Irradiation. *Brain Behav. Immun.* **1997**, *11*, 273–285. [[CrossRef](#)]
86. Kim, J.-I.; Jeon, S.G.; Kim, K.A.; Kim, J.-J.; Song, E.J.; Jeon, Y.; Kim, E.; Lee, K.B.; Kwak, J.H.; Moon, M. Platycodon grandiflorus Root Extract Improves Learning and Memory by Enhancing Synaptogenesis in Mice Hippocampus. *Nutrients* **2017**, *9*, 794. [[CrossRef](#)]
87. Rivera, I.; Capone, R.; Cauvi, D.M.; Arispe, N.; De Maio, A. Modulation of Alzheimer's amyloid beta peptide oligomerization and toxicity by extracellular Hsp70. *Cell Stress Chaperones* **2018**, *23*, 269–279. [[CrossRef](#)]
88. Heissig, B.; Rafii, S.; Akiyama, H.; Ohki, Y.; Sato, Y.; Rafael, T.; Zhu, Z.; Hicklin, D.J.; Okumura, K.; Ogawa, H.; et al. Low-dose irradiation promotes tissue revascularization through VEGF release from mast cells and MMP-9-mediated progenitor cell mobilization. *J. Exp. Med.* **2005**, *202*, 739–750. [[CrossRef](#)]
89. Jansen, H.; Meffert, R.; Birkenfeld, F.; Petersen, W.; Pufe, T. Detection of vascular endothelial growth factor (VEGF) in moderate osteoarthritis in a rabbit model. *Ann. Anat. Anat. Anz.* **2012**, *194*, 452–456. [[CrossRef](#)]
90. Sanchez, A.; Wadhvani, S.; Grammas, P. Multiple neurotrophic effects of VEGF on cultured neurons. *Neuropeptides* **2010**, *44*, 323–331. [[CrossRef](#)]
91. Mesquita, S.D.; Louveau, A.; Vaccari, A.; Smirnov, I.; Cornelison, R.C.; Kingsmore, K.M.; Contarino, C.; Onengut-Gumuscu, S.; Farber, E.; Raper, D.; et al. Functional aspects of meningeal lymphatics in ageing and Alzheimer's disease. *Nature* **2018**, *560*, 185–191. [[CrossRef](#)] [[PubMed](#)]
92. Stott, D.J.; Rodondi, N.; Kearney, P.M.; Ford, I.; Westendorp, R.G.J.; Mooijaart, S.P.; Sattar, N.; Aubert, C.E.; Aujesky, D.; Bauer, D.C.; et al. Thyroid Hormone Therapy for Older Adults with Subclinical Hypothyroidism. *N. Engl. J. Med.* **2017**, *376*, 2534–2544. [[CrossRef](#)] [[PubMed](#)]
93. Liang, C.-C.; Park, A.Y.; Guan, J.-L. In vitro scratch assay: A convenient and inexpensive method for analysis of cell migration in vitro. *Nat. Protoc.* **2007**, *2*, 329–333. [[CrossRef](#)] [[PubMed](#)]
94. Vorhees, C.V.; Williams, M.T. Morris water maze: Procedures for assessing spatial and related forms of learning and memory. *Nat. Protoc.* **2006**, *1*, 848–858. [[CrossRef](#)]
95. Livak, K.J.; Schmittgen, T.D. Analysis of relative gene expression data using real-time quantitative PCR and the 2(-Delta Delta C(T)) Method. *Methods* **2001**, *25*, 402–408. [[CrossRef](#)]

